Biomedical Microdevices 5:2, 163–168, 2003

Therapeutic Micro and Nanotechnology:

Section Editor Dr Tejal Desai

Tension Development and Nuclear Eccentricity in Topographically Controlled Cardiac Syncytium

Emilia Entcheva[1,2] and Harold Bien[1]*

[1] Department of Biomedical Engineering and Department of Physiology and Biophysics, Stony Brook University

[2] Department of Biomedical Engineering, Stony Brook University, HSC T18-030, Stony Brook, NY 11794-8181

E-mail: emilia.entcheva@sunysb.edu

Abstract. **The goal of this study was to use topographic control by microfabricated scaffolds with 3-dimensional surfaces to induce active tension development and enhanced contractility in engineered cardiac syncytium (a high density cardiac cell structure with reconstituted cell-to-cell connections and synchronized tissue-like behavior). Deeply microgrooved (feature height 50μm) elastic scaffolds were designed using polydimethylsiloxane molding, and neonatal rat cardiomyocytes were grown on them to confluency. Engineered cardiac cell constructs on the topographically modified (T) scaffolds showed higher order of intra and intercellular organization (fiber-like structures) compared to those grown on various flat surfaces (F), and developed self-organized persisting electrical and mechanical activity. These structural and functional changes were accompanied by a statistically significant ($p < 0.001$) increase in nuclear eccentricity (mean $\pm$ S.E.: $0.79 \pm 0.01, n = 137$ in T vs. $0.64 \pm 0.01, n = 863$ in F), and a preferential nuclear orientation, deviating from the axis of the grooves at a shallow angle. The orientation of the nuclei correlated well with the actin fiber arrangement in the T-samples, as well as with the direction of maximum displacement. Topography-induced nuclear deformation, a sign of tension development, implies further functional changes in transcription and cell signaling. In conclusion, we demonstrate topographic control of electromechanics in engineered cardiac syncytium, without external mechanical or electrical stimulation. These findings suggest a possibility to use controled microenvironments in the design of biological autonomous force generators with reconstituted excitable tissue.**

Key Words. **topography, cardionyocytes, microfabrication, cardiac tissue engineering**

Introduction

Engineering functional cardiac tissue *in vitro* is an ambitious actively pursued endeavor (Zimmermann et al., 2002; Fink et al., 2000). Along with the obvious clinical benefit of the eventual final product (tissue repair for the human heart), a few potential *in vitro* applications seem of no lesser importance and interest. One of them is the use of successfully engineered cardiac tissue for drug development—target screening and validation of potential pharmacological compounds (Nave et al., 2002). Another interesting application of engineered excitable and contractile tissue (such as cardiac muscle) stems from its potential (Kakugo et al., 2002) to be used as a biological machine for performing useful work with high efficiency. Achieving the desired functionality through minimum external intervention, relying on the self-organizing properties of biological matter, is a laudable, yet insufficiently explored approach.

Previous research has demonstrated the feasibility of perturbing cell function and survival by controlling the cellular microenvironment (Chen et al., 1997). In the context of cardiac tissue, cell patterning and guidance have been applied by manipulating the extracellular matrix (ECM) proteins: micropatterns of desired shape and size (Rohr et al., 1991) or oriented gels (Simpson et al., 1994) invoked reciprocal structural and functional cellular responses. Most of these studies dealt with 2-dimensional preparations. Topographic control within a true 3-dimensional setting is expected to promote higher order of organization. Several groups (Clark et al., 1990), including one (Deutsch et al., 2000) dealing with primary cardiac cells at low density, have pointed out the ability of the cells to make use of topographic features for out-of-plane support. Our goal in this study was to engineer cardiac syncytium on microfabricated topographically complex scaffolds. We anticipated that the 3-dimensional landscape, combined with such a well-connected network of excitable contractile cells would bring about unique system behavior, including the promotion of organized electrical and mechanical activity. We characterize several aspects of the topography-induced structural and functional changes, focusing on nuclear

*Corresponding author.

deformation as a consequence of the increased level of organization and enhanced inherent mechanical activity, and with important implications for re-programming the cells.

This work has been presented before in an abstract form (Entcheva and Bien, 2002).

Methods

Scaffolds and topography

Several different scaffold materials were used in this study. As flat rigid surfaces for cell growth we used glass and polyvinylchloride (both from VWR, West Chesler, PA), polydimethylsiloxane (PDMS) and cellulose-acetate (CA) surfaces. PDMS scaffolds (Sylgard 184 from Dow Corning, Midland, MI) were prepared in the usual ratio of 1:10 of curing agent to elastomer and baked for 2 hours at 60 °C. CA membranes were prepared from cellulose acetate, triethyl citrate and acetone (all from Aldrich, St. Louis, MD) and let form thin membranes over 4–5 hours. To investigate the effects of topography on cellular growth and function, PDMS scaffolds were constructed by molding from premanufactured micro-grooved masters. The resultant scaffold surface had regularly spaced features of uniform height with trapezoidal grooves and triangular ridges. The features, explored here, are significantly larger than those examined in previous studies (Deutsch et al., 2000). Cross sections of scaffolds were imaged under conventional microscopy to confirm topographical features (Figure 1A).

Cardiac syncytium

Cardiomyocytes were cultured from neonatal rat hearts as described elsewhere (Entcheva et al., 2000). Briefly, cardiomyocytes were isolated from the ventricles of 3-day old rats by enzymatic digestion with trypsin and collagenase. Cells were plated at high density (0.9×10^6 cells per ml) onto fibronectin-coated scaffolds to allow the reconstitution of cell-to-cell contacts and the establishment of a functional syncytium. Electrical cell-to-cell connections were confirmed by gap junctional (Connexin 43) staining (Bien et al., 2002) and assessment of multicellular behavior. The engineered cell constructs (Figure 1B) were maintained at 37 °C with 5% CO_2 in medium 199 supplemented with 2% fetal bovine serum.

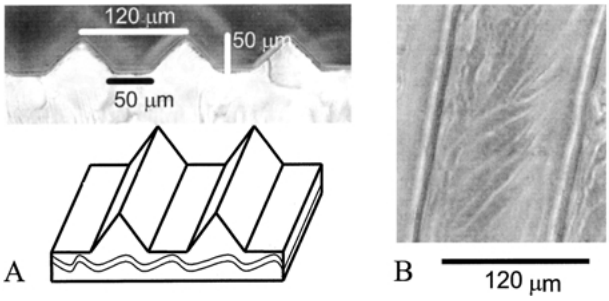

Fig. 1. Geometry of topographically complex scaffolds constructed by molding from micro-grooved masters, and cardiac cell network grown on the scaffolds.

Electromechanical measurements

Electromechanical measurements were performed at day 3–6 after culturing, under perfusion with oxygenated Tyrode's solution at 32–35 °C. Intracellular calcium levels were determined using a ratiometric fluorescence measurement technique, as described previously (Bien et al., 2002). Cells were stained with 10 μm of the calcium-sensitive dye Fura-2 (Molecular Probes, Eugene, OR) at room temperature for 20 minutes, and unincorporated stain was washed out for another 20 minutes. Samples were then imaged using an inverted fluorescence microscope (Nikon 20× Fluor objective, NA 0.75) with excitation at 365 nm and 380 nm, and the fluorescence intensity determined through a 510 nm band-pass filter using a photo-multiplier detector (IonOptix, Milton, MA). Cell length was tracked simultaneously at long wavelengths using fast (250 Hz) imaging with a CCD camera and software video-trackers of cell edges along the axis of deformation. Movies of multicellular deformation were recorded using a Nikon Coolpix 950 camera attached to the eyepiece of the microscope.

Fluorescent labeling and confocal microscopy

At day 7 of culture cardiomyocytes were fixed in 3.7% formaldehyde and permeabilized with 0.02% Triton-X 100. Cells were co-stained with phalloidin-Alexa 488 (Molecular Probes) for F-actin and with TOTO-3 (Molecular Probes) for nuclei. Samples were then mounted on a glass slide with VectaShield (Vector Laboratories, Burlingame, CA) and imaged with a confocal scanning laser microscope BioRad Radiance 2000 with a 60× objective (N.A. 1.4), excited simultaneously at 488 nm for actin and 637 nm for TOTO-3. Emission at 535 nm was mapped to the green channel and 680 nm to the blue channel in a 24-bit RGB format containing $1{,}024 \times 1{,}024$ pixels representing 195 μm × 195 μm area. Only the blue channel, reflecting TOTO-3 staining, was used for nuclear analysis as an intensity scale.

Automated analysis of nuclear morphology

We developed and applied an automated technique for nuclear morphology analysis using the confocal images. After thresholding a grayscale nuclear image using Otsu's method (Otsu, 1979), median spatial filtering

was applied to clean nuclear edges, and the whole image was segmented into connected regions. Based on criteria including region size, ''solidity'' and degree of concavity, individual nuclei were discriminated from noise. Ellipsoidal shape was automatically fitted around each identified nucleus, and the parameters (size, eccentricity, orientation) of this (ellipsoidal) envelope were further used in the analysis. The algorithm was implemented using the Image Processing Toolbox in Matlab (Mathworks, Novi, MI), and validated by comparison to manually selected and characterized nuclei.

Results

In this study we engineered cardiac tissue-like constructs on different materials, specifically seeking to quantify the effects of topography on the cell construct structure and function. All materials used were biocompatible and optically clear, allowing easy cell visualization and functional microscopy studies. Unlike previous attempts at cell alignment through patterning (Rohr et al., 1991) or orientation (Simpson et al., 1994) of the ECM, here we employed true 3-dimensional structures (deep wide microgrooves), and assessed self-organized syncytial behavior.

Cardiomyocytes grown on topographically complex scaffolds exhibited a highly organized pattern of growth and attachment (Figure 1B) compared to flat scaffolds. Structural changes were obvious in the actin arrangement-cells in the grooves formed *in vivo*-like fiber structures, making use of the out-of-plane lateral support and extending in the spaces between the triangular peaks, and orienting themselves at a shallow angle with respect to the long axis of the grooves (Figure 2A), whereas cardiomyocytes grown on flat surfaces spread out in all directions, with low order of cytoskeletal organization (Figure 2B). Additional structural changes included a larger size for the cells on the topographically complex surfaces, and a more pronounced sarcomere pattern along the actin fibers.

The cytoskeletal re-arrangement and changes in cytoarchitecture in response to topography were accompanied by functional changes. Constructs on topographically modified scaffolds developed self-organized synchronous contractions after day 3 in culture. The persistence and the magnitude of these contractions were much more pronounced than similar activity observed sporadically on any of the flat surfaces. Cell-driven deformation of the underlying scaffold was observed (movies available). The frequency range of the observed spontaneous activity was 0.8–2.5 Hz at 32–37 °C. Representative recordings are shown in Figure 3, where the frequency of the inherent activity is about 1 Hz. The cell strain was recorded and evaluated along the axis of maximum displacement, which was close to the axis of actin fiber orientation, depicted in Figure 2.

Visually, the nuclei of cells grown on topographically complex scaffolds appeared more elongated (Figure 1B).

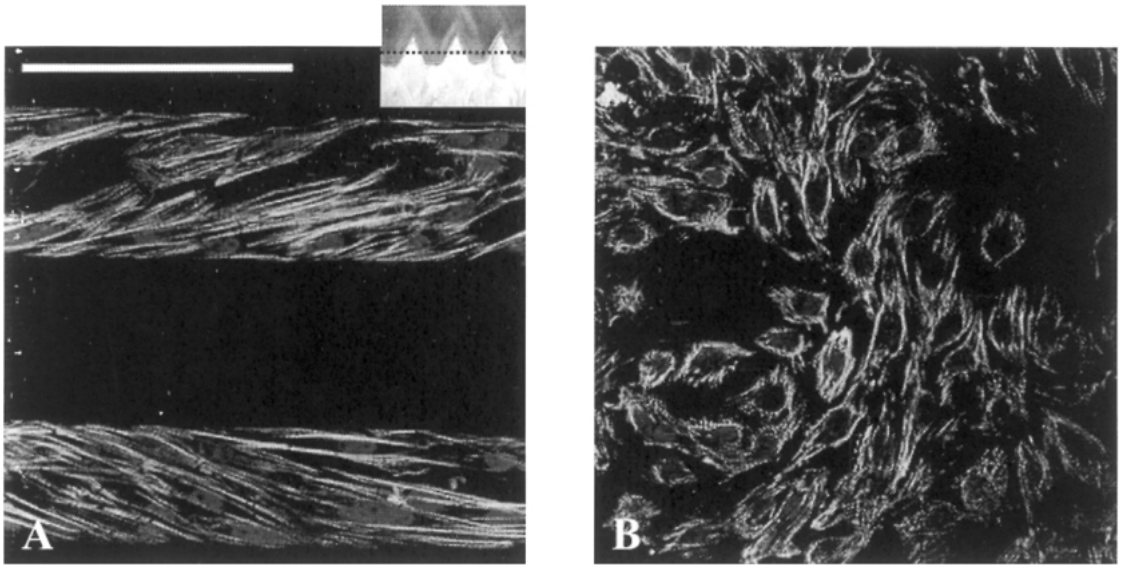

Fig. 2. *Engineered cell constructs on topographically complex scaffolds exhibit highly organized cytoskeleton with efficient use of topographical features for attachment. Confocal image of cardiomyocytes grown on microgrooved PDMS (A) and flat PDMS (B) scaffolds. Intracellular structures have been labeled with phalloidin-Alexa 488 and TOTO-3, a nuclear stain. Note the higher order of organization of the contractile fibers in (A), running from side to side in the grooves. Scale bar is 100 μm. Inset shows schematically the position of a confocal slice with respect to the scaffold structure (exaggerated vertical dimension).*

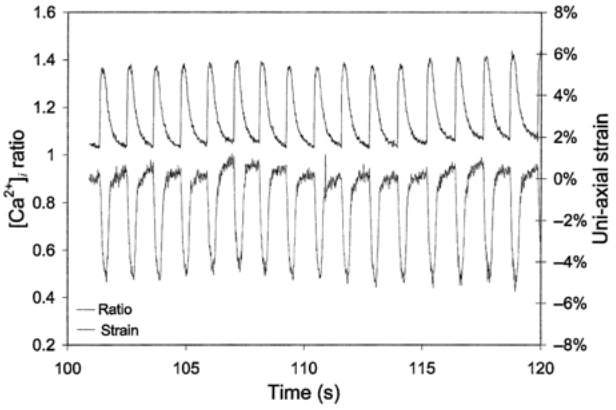

Fig. 3. Engineered cell constructs on topographically complex scaffolds exhibit self-organized persistent electrical and mechanical activity without external load / stimulation. Intracellular calcium, $[Ca^{2+}]_i$, upper trace was assessed using a ratiometric fluorescence measurement with a calcium-responsive dye Fura-2, excited at 365 nm and 380 nm. Higher ratios correlate with higher intracellular calcium concentrations. Cell length lower trace was measured using fast computer-aided videomicroscopy. Uniaxial strain was computed as the difference between the initial (diastolic) length and current length, divided by the diastolic length.

This was definitively demonstrated by using a custom developed automated software to determine nuclear morphology in the engineered constructs. Summary of the data is presented in Figure 4. The mean nuclear eccentricity of cardiomycytes grown in a syncytium on a flat surface was found to be very close to 0.64 ± 0.01 (mean S.E.), $n = 847$, regardless of scaffold material.

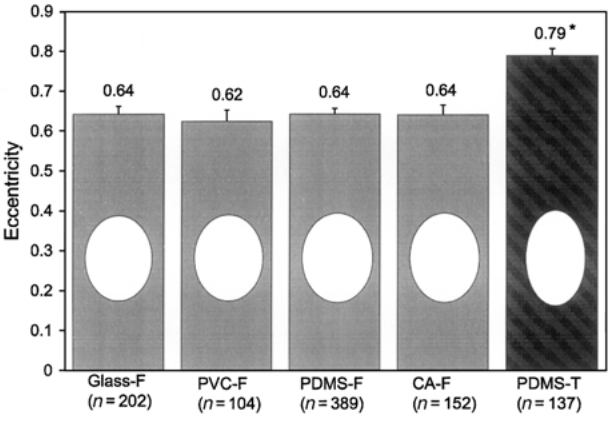

Fig. 4. Engineered cell constructs on topographically complex scaffolds exhibit greater nuclear eccentricity ($p < 0.001$). Eccentricity of 0 indicates a perfect circle, eccentricity of 1—a line. The examined scaffold materials include flat (F) PDMS, PVC, CA and glass, and topographically modified (T) PDMS. Error bar indicate 95% confidence intervals, and the ellipses are a graphical representation of the mean nuclear geometry scaled proportionally to the mean major and minor axis lengths.

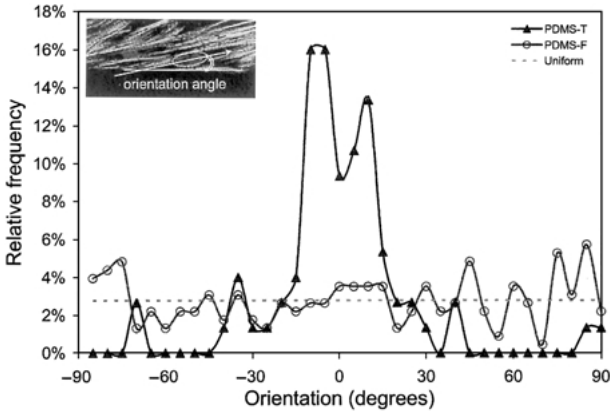

Fig. 5. Engineered cell constructs on topographically complex scaffolds exhibit preferential nuclear orientation ($p < 0.001$), consistent with the orientation of the contractile fibers (Figure 2) and the direction of maximum strain (Figure 3). The inset illustrates the definition of the orientation angle: between the major axis of a fitted ellipse around a nucleus and the horizontal axis of the confocal image (before angle calculations, coordinate transformation was applied to align topographical features with the x-axis). Dashed line indicates expected relative frequency for random orientation (uniform distribution). Frequency data were binned in 5-degree increments. Cell nuclei on topographically modified scaffolds deviated significantly from the uniform distribution (see also Table 1).

Statistically significant increase in nuclear eccentricity to $0.79 \pm 0.01, n = 137$, was observed in the cells on topographically modified PDMS surfaces. These nuclei were longer and narrower than the control ones (major axis 13.5 ± 0.25(T) vs. 12.7 ± 0.12 (F) and minor axis 7.6 ± 0.13 (T) vs. 9.3 ± 0.08 (F)). Given the large width of the grooves employed with respect to cell dimensions, it is unlikely that nuclear deformation occurred as a result of geometry confinement, or simple orientation along the grooves (see next paragraph).

Nuclear morphological changes were accompanied by development of a preferential orientation (Figure 5). While orientation of cell nuclei on flat substrates (regardless of material) did not deviate significantly from the random distribution, cell nuclei on topographically modified surfaces had a preferential orientation, $p < 0.001$, chi-square results presented in Table 1. The range of orientation angles, followed by the oriented nuclei, was $-20/+20$ degrees with respect to the groove direction, with a drop at 0 degrees. This was consistent with the preferential direction of actin fiber orientation and the direction of developed maximum contractions.

Same sets of data were used for calculations of nuclear eccentricity and nuclear orientation. Data were collected from 25 scaffolds for flat (different materials) and seven scaffolds for topographically modified PDMS.

Table 1. *Chi-square test for deviation of nuclear orientation on different surfaces (examined in Figure 4) from the uniform (non-biased) distribution. Only topographically complex scaffolds promoted ($p < 0.001$) preferential orientation of the nuclei within $-20/+20$ degrees from the axis of the surface grooves (see also Figure 5)*

	Glass-F	PVC-F	PDMS-F	CA-F	PDMS-T
Number of nuclei	202	104	389	152	137
χ^2	34	44	36	41	144
Degrees of freedom	35	33	35	35	28
p	0.52	0.10	0.43	0.22	< 0.001

Discussion and Conclusions

This study demonstrates topographic control of cardiac electromechanics, as assessed by structural changes on the single cell and on the network (tissue) level, as well as functional changes in engineered cardiac syncytium on deeply microgrooved scaffolds.

We report three pieces of evidence for topography effects on engineered cardiac constructs. First, cytoskeletal rearrangement and alignment of actin stress fibers of cells grown on topographically complex T-constructs compared to F-constructs was observed. More mature looking (sarcomered) cytoskeleton was characteristic for the T-constructs. Cell (actin fibers) and nuclear orientation come as no surprise in response to guiding topography (Clark et al., 1990). The interesting finding here is the deviation from the axis of the grooves and the formation of twisted fiber-like structures, mimicking real heart tissue.

The second, functional result of scaffold topography, deals with the promotion of synchronous persistent electrical and mechanical activity. The induction of topographically driven functional changes, observed here, is in concert with our previous results (Bien et al., 2002), where a statistically significant increase in the magnitude of intracellular calcium transients was found for cells on topographically modified vs. flat surfaces. Calcium is the triggering signal for contraction in cardiac myocytes; hence our overall results support the idea of topography effects on excitability and contractility.

Finally, we quantify nuclear morphology and orientation. In contrast to a tightly maintained nuclear shape in cell networks on flat substrates, the cells in T-constructs exhibited higher nuclear eccentricity. Furthermore, the nuclei of these cells followed the preferential alignment of the stress fibers. Previous studies have clearly demonstrated nuclear deformation as a result of external mechanical stretch (Maniotis et al., 1997; Arnoczky et al., 2002). We believe that the changes in nuclear morphology, reported here, result from combined structural and functional effects. The latter are associated with tension developed within the highly active T-constructs.

The exact mechanism of these topography-mediated phenomena is unknown; below we propose a framework

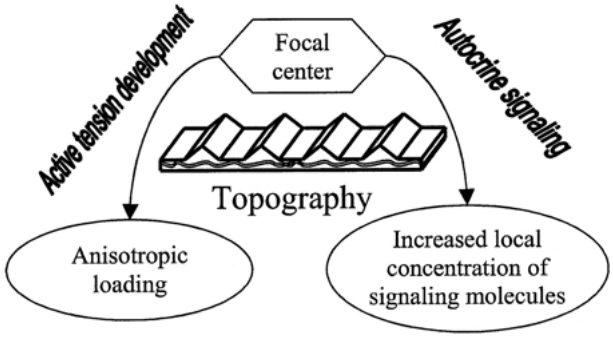

Fig. 6. *Proposed pathways (mechanical and biochemical) for topography-induced enhancement and synchronization of electro-mechanical activity in cardiac cell constructs on the microgrooved scaffolds.*

of possible pathways for the evolution and facilitated synchronization of electro-mechanical activity in the T-constructs. As shown in Figure 6, a focal center (FC) of spontaneous contractile activity is a necessary starting point. Pacemaking sites do occur in the cultured neonatal rat ventricular preparation, and we have observed them on flat as well as on microgrooved surfaces. The process of propagation and synchronization of this spontaneously occurring activity requires a high degree of connectivity (i.e., a syncytial structure). Furthermore, we propose at least two plausible topography-related spatial mechanisms of synchronization and reinforcement of this activity. First, through a ''mechanical'' pathway the FC activity resembles external tensile forces on neighboring cells, attached to the 3-dimensional structures. Alternatively, the reaction forces from cellular attachment sites of contracting cells also mimic external tension. Even though a similar interaction of forces does exist in the F-constructs of well-connected cells, the key difference (uniquely brought about by topography) is the anisotropic nature of the applied loads (due to a preferential orientation) and the periodic 3-dimensional supports, which further facilitate the intrinsic force development. This periodic load can activate initially quiescent cells through mechano-sensitive channels or other mechanotransduction mechanisms (i.e., elevated intracellular Ca^{2+} levels). A second, ''biochemical''

pathway is believed to exist through autocrine signaling, i.e., the release of growth factors, hormones etc. by the active FC cells and their effect on initially quiescent neighboring cells. There is extensive evidence in support of this scenario following mechanical activity in cardiomyocyte networks (Ruwhof et al., 2000; van Wamel et al., 2001). The topography contribution in this regard, for our particular configuration, could be the provision of a somewhat confined space (deep grooves) to reinforce these microenvironment effects.

The development of synchronous mechanical activity and the anisotropic nature of the intrinsic stretch lead to increased nuclear eccentricity by previously established mechanotransduction pathways (Maniotis et al., 1997). Nuclear deformation then can affect the overall cell function through gene expression and transcriptional mechanisms (Thomas et al., 2002) by leading to further structural and mechanical changes.

In conclusion, we demonstrate in this study that scaffold topography can induce unique functional changes in a well-connected network of cardiomyocytes. This finding, together with further elucidation of the mechanisms involved, could serve as a guiding point in tissue engineering efforts and the design of autonomous mechanical structures out of excitable cells.

Acknowledgments

We would like to thank Lihong Yin and David Colflesh for help with the cell culture and the confocal imaging, respectively.

References

S.P. Arnoczky, M. Lavagnino, J.H. Whallon, and A. Hoonjan, J. Orthop. Res. **20**, 29–35 (2002).

H. Bien, L. Yin, and E. Entcheva, Proceedings of IEEE Engineering in Medicine and Biology Society and BMES Annual Conference, October 10, Houston, TX (2002).

C.S. Chen, M. Mrksich, S. Huang, G.M. Whitesides, and D.E. Ingber, Science **276**, 1425–1428 (1997).

P. Clark, P. Connolly, A.S. Curtis, J.A. Dow, and C.D. Wilkinson, Development **108**, 635–644 (1990).

J. Deutsch, D. Motlagh, B. Russell, and T.A. Desai, J. Biomed. Mater. Res. **53**, 267–275 (2000).

E. Entcheva, and H. Bien, Third Annual Conference BioMEMs and Biomedical NanoTech World 2002, Columbus, OH, 2002.

E. Entcheva, S.N. Lu, R.H. Troppman, V. Sharma, and L. Tung, J. Cardiovasc. Electrophysiol. **11**, 665–676 (2000).

C. Fink, S. Ergun, D. Kralisch, U. Remmers, J. Weil, and T. Eschenhagen, Faseb. J. **14**, 669–679 (2000).

A. Kakugo, S. Sugimoto, J.P. Gong, and Y. Osada, Adv. Mater. **14**, 1124–1126 (2002).

A.J. Maniotis, C.S. Chen, and D.F. Ingber, Proc. Natl. Acad. Sci. USA **94**, 849–854 (1997).

B.T. Nave, M. Becker, V. Roenicke, and T. Henkel, Drug Discov. Today **7**, 419–425 (2002).

N. Otsu, IEEE Trans. Sys. Man. Cyber. **9**, 62–66 (1979).

S. Rohr, D. Shoelly, and A. Kleber, Circ. Res. **68**, 114–130 (1991).

C. Ruwhof, A.E. van Wamel, J.M. Egas, and L.A. van der, Mol. Cell Biochem. **208**, 89–98 (2000).

D.G. Simpson, L. Terracio, M. Terracio, R.L. Price, D.C. Turner, and T.K. Borg, J. Cell. Physiol. **161**, 89–105 (1994).

C.H. Thomas, J.H. Collier, C.S. Sfeir, and K.E. Healy, Proc. Natl Acad. Sci. USA **99**, 1972–1977 (2002).

A.J. van Wamel, C. Ruwhof, L.E. van der Valk-Kokshoom, P.I. Schrier, and L.A. van der, Mol. Cell. Biochem. **218**, 113–124 (2001).

W.H. Zimmermann, K. Schneiderbanger, P. Schubert, M. Didie, F. Munzel, J.F. Heubach, S. Kostin, W.L. Neuhuber, and T. Eschenhagen, Circ. Res. **90**, 223–230 (2002).